Available online at www.sciencedirect.com
SCIENCE DIRECT®
Journal of Sound and Vibration 274 (2004) 939–951
JOURNAL OF SOUND AND VIBRATION
www.elsevier.com/locate/jsvi

Application of an active controller for reducing small-amplitude vertical vibration in a vehicle seat

Jian-Da Wu*, Rong-Jun Chen

Department of Mechanical and Automation Engineering, Da-Yeh University, 112 Shan-Jiau Road, Da-Tsuen, Changhua 515, Taiwan, ROC

Received 7 October 2002; accepted 2 June 2003

Abstract

This report describes the principle and application of active vibration control (AVC) for reducing undesired small-amplitude vertical vibration in the driver's seat of a vehicle. Three different control algorithms are implemented and compared in the experimental investigation. Apart from adaptive control and robust control, a hybrid control algorithm consisting of a combination of an adaptive controller with a filtered-x least mean squares (FXLMS) algorithm and a feedback structure with a robust synthesis theory for obtaining fast convergence and robust performance are proposed. A frequency domain technique is used for achieving the control plant identification and controller design. All of the proposed AVC controllers are implemented in a digital signal processor (DSP) platform, using a finite impulse response (FIR) filter for real-time control. A characteristic analysis and experimental comparison of three control algorithms for reducing the small amplitude vertical vibration in a vehicle seat are also presented in this paper.

1. Introduction

Almost every possible mechanism for generating noise and vibration is present in a vehicle. In recent years, vehicle noise, vibration and harshness (NVH) have attracted greatly intensified attention. Vibration transfers to the seat and the human body are known to be a major source of discomfort for the driver. The vibration source is often caused by the internal combustion engine and road conditions. Vibration transfer is an important problem having a significant influence on

*Corresponding author. Tel.: +886-4-851-1888; fax: +886-4-851-1666.
E-mail address: jdwu@mail.dyu.edu.tw (J.-D. Wu).

0022-460X/$ - see front matter © 2003 Elsevier Ltd. All rights reserved.
doi:10.1016/S0022-460X(03)00655-2

human fatigue and safety [1–4]. In general, there are three approaches to minimize unwanted vibrations in the structure of the driver's seat of an automobile, i.e., passive, semi-active and active vibration control. The passive elements include engineered pneumatic suspension, a hydraulic damper and shock absorbers. The performance of a passive vibration control system is limited because the parameter of the system is usually fixed. In addition, semi-active systems such as magneto-rheological (MR) fluid dampers and electro-rheological (ER) fluid dampers can also be used to absorb the vibration in the driver's seat. However, semi-active dampers do not provide a power source for control force. They normally use a controlled damper to remove energy from the suspension system, as in the most well-known control algorithm, 'the Skyhook controller' [5–7]. However, active vibration control (AVC) serves as a promising alternative to conventional passive control and semi-active approaches in that it provides advantages such as improving the performance of small-amplitude vibration and time varying systems.

Interest in active control has grown significantly, having advanced with the progress of digital signal-processing technology and hardware in the last two decades [8–10]. Many sophisticated control algorithms and techniques have been implemented on digital signal processor (DSP) platforms for practical applications. In particular, AVC of a platform with a synthesis vibration source has been extensively investigated, both theoretically and experimentally. In active-control structures, adaptive feedforward control has become the most widely used method for reducing noise and vibration when a reference source is available. For an adaptive control, the filtered-x least mean squares (FXLMS) algorithm is well-known, having been used extensively in many applications such as adaptive active noise cancellation and active vibration control [11–13]. However, in a practical implementation of the FXLMS algorithm, convergence speed often limits AVC system performance when a vibration source or a control plant is varied, such as in cases of vibration from normal engine slew rates or during gear shifting, because the learning process of the adaptive algorithm fails to respond fast enough to the changing operation conditions. Meanwhile, in a control system, plant uncertainty also is one of the major factors that can affect the performance and stability of a system [14,15]. Plant uncertainty may be caused by physical conditions such as engine speed or a change in road condition. Such uncertainty may also be caused by errors in system modeling, measurement, and computation. Changes in physical conditions and errors lead to deviations in the plant, thereby affecting the robustness of the control systems.

In the present study, a hybrid control algorithm consisting of a combination of adaptive control with the FXLMS algorithm and a feedback structure with a robust synthesis theory for obtaining fast convergence and robust performance is proposed for reducing small-amplitude vertical vibration in the driver's seat of an automobile. In controller design, the H_∞ feedback robust controller is used for overcoming a plant with structural uncertainties. Additive uncertainty weights are used to account for the external disturbance and the unmodelled dynamics in the design procedure. The proposed hybrid controller is implemented on a TMS320C32 DSP platform. Experimental investigations are implemented to compare the attenuation performance of a traditional adaptive controller, a pure H_∞ feedback controller and the proposed hybrid robust controller.

2. Control algorithms of AVC system

2.1. Adaptive control structure

The FXLMS is a well-known algorithm often used to deal with active noise and vibration control in cases when the reference source, such as engine revolution, is measurable [12,13]. In Fig. 1, the block diagram is a multi-channel control system with K reference signals, M secondary sources and I error sensors. The reference signal $x(n)$ is supplied to the control plant which causes the structural vibration. This signal is also provided to an adaptive controller $W(z)$ which adapts slowly when compared to the rate of change of reference signal. In the adaptive filters, the reference signals to derive the control output signals $y(n)$ are obtained by

$$y_m(n) = \sum_{m=1}^{3} \sum_{k=1}^{3} w_{mk}^{\mathrm{T}}(n) * x_k(n) \quad m,k = 1,2,3, \tag{1}$$

where $w(n)$ is the vector of the $M \times K$ filter weighting coefficient at the nth sample time, $x(n)$ is the $K \times 1$ vector of past reference signals and $*$ is the convolution operator. The control signals can be supplied to the active mounts which apply the counter acting force to the device. The impulse responses of the dynamic secondary paths $\hat{S}(z)$ are considered from the Mth secondary sources to the Mth error signals. There are $M \times I$ different transfer paths between each secondary source and each error signal, all of which must be modelled and used K times to generate the array of filtered reference signals required for the adaptive algorithm. The filtered referenced signals $x'(n)$ can be written as

$$x'_k(n) = \sum_{m=1}^{3} \hat{S}_{im} * x_k(n) \quad i,m,k = 1,2,3. \tag{2}$$

The error signals $e(n)$ measured by the ith sensor can be expressed as

$$e_i(n) = d_m(n) - \sum_{m=1}^{3} S_{im}(n) * y_m(n) \quad i,m = 1,2,3. \tag{3}$$

The objective of the controller is to minimize the mean-square error. The filtered-x LMS algorithm is widely used to adapt the coefficients of an FIR digital filter for vibration cancellation.

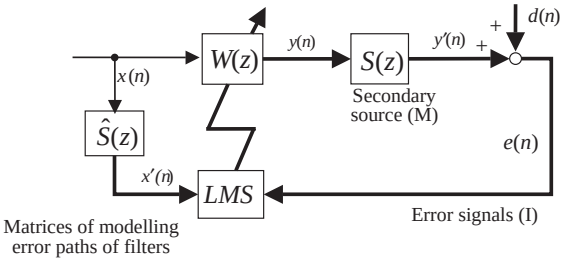

Fig. 1. Block diagram of MIMO AVC system using filtered-x LMS algorithm.

This algorithm can be written as

$$w_{mk}(n+1) = w_{mk}(n) - \mu \sum_{m=1}^{3} x'_{\mathrm{kim}}(n) * e_i(n) \quad m,k,i = 1,2,3, \tag{4}$$

where $x'(n)$ is the $K \times IM$ matrix of filtered reference signals, $e(n)$ is the $I \times 1$ vector of error signals and μ is the convergence coefficient that affects the stability and convergence rate.

2.2. H_∞ robust structure

In practical application, it is often difficult to detect the properties of the vibration source in a control system [13]; therefore, an H_∞ feedback controller is often used in such a situation. Active control systems are generally designed for a disturbance rejection problem, for which a generalized system is shown in Fig. 2. The system matrix can be defined by

$$\begin{bmatrix} z \\ v \end{bmatrix} = \begin{bmatrix} G_{11} & G_{12} \\ G_{21} & G_{22} \end{bmatrix} \begin{bmatrix} w \\ u \end{bmatrix}, \tag{5}$$

$$u = -Kv, \tag{6}$$

where the signal z reflects the objectives, v denotes the measurement signals, w comprises all exogenous inputs, u denotes the controller output signals and K is the feedback controller. In this study, a mixed sensitivity problem with structural uncertainty in a plant is shown in Fig. 3. The system model can be expressed by

$$\begin{bmatrix} d(n) \\ z(n) \\ v(n) \end{bmatrix} = \begin{bmatrix} G_{11}(z) & G_{12}(z) & G_{13}(z) \\ G_{21}(z) & G_{22}(z) & G_{23}(z) \\ G_{31}(z) & G_{32}(z) & G_{33}(z) \end{bmatrix} \begin{bmatrix} m(n) \\ w(n) \\ u(n) \end{bmatrix}. \tag{7}$$

The H_∞ feedback structure in our design includes two weighting functions (low-pass and high-pass) and two plant functions, shown in Fig. 4. The weighting functions are chosen to shape the frequency response of the nominal plant to achieve the loop shape. The state-space model of the

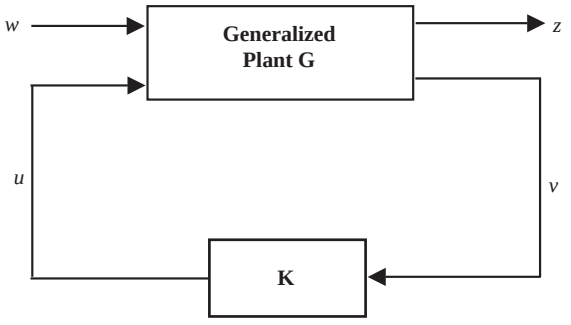

Fig. 2. Block diagram of generalized system.

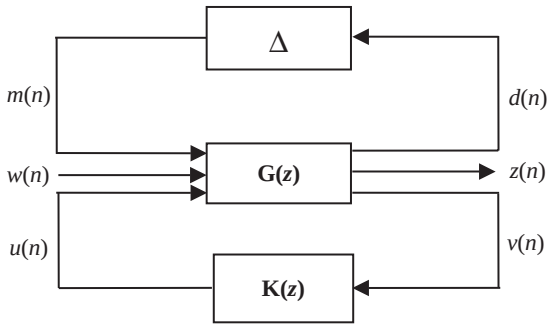

Fig. 3. Feedback control system with plant uncertainty.

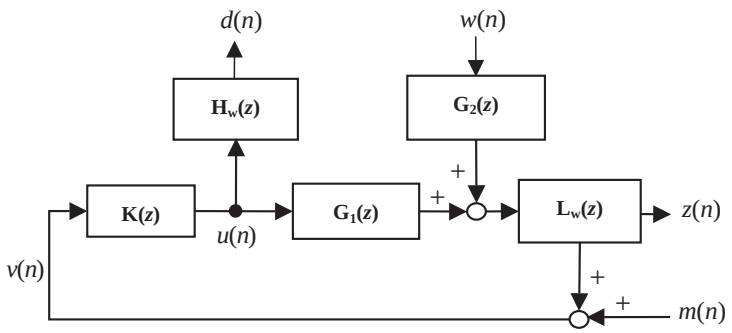

Fig. 4. Block diagram of mixed sensitivity system with disturbance plant uncertainty.

mixed sensitivity problem can be expressed as

$$\begin{aligned} d(n) &= H_w(z)u(n), \\ z(n) &= L_w(z)[G_1(z)u(n) + G_2(z)w(n)], \\ v(n) &= G_1(z)u(n) + m(n)I + G_2(z)w(n). \end{aligned} \tag{8}$$

In the H_∞ controller design, two weighting functions must be determined, one being the high-pass function $H_w(z)$ used to derive the desired performance, the other being the low-pass function $L_w(z)$ used to obtain robust stabilization in the control system. This system is assumed to be a linear controller, for which the control input $u(n)$ is given by

$$u(n) = -K(z)v(n). \tag{9}$$

From Eqs. (6)–(8), $u(n)$ and $v(n)$ are eliminated to obtain

$$\begin{bmatrix} d(n) \\ z(n) \end{bmatrix} = \begin{bmatrix} M_{11}(z) & M_{12}(z) \\ M_{21}(z) & M_{22}(z) \end{bmatrix} \begin{bmatrix} m(n) \\ w(n) \end{bmatrix}. \tag{10}$$

The transfer functions from $z(n)$ to $w(n)$ can be expressed as

$$\begin{aligned} T_{z,w}(z) &= M_{ij}(z)\big[G_{ij}(z), K(z)\big] \\ &= G_{ij}(z) + G_{i3}(z)K(z)[I - K(z)G_{33}(z)]^{-1}G_{3j}(z) \quad i,j = 1,2. \end{aligned} \tag{11}$$

The purpose of the H_∞ theory is to search for the feedback controller $K(z)$ which minimizes $\|T_{z,w}(z)\|_\infty$, which can be equivalently expressed as

$$\text{minimum} \sup_{\substack{-\infty \leqslant \omega \leqslant \infty \\ \omega \neq 0}} \|T_{z,w}(z)\|. \tag{12}$$

In practice it is difficult to design an optimal controller. The proper transfer function $T_{z,w}(Z)$ which satisfies the infinity norm on controller $K(z)$ can be found. Generally speaking, if the transfer function $T_{z,w}(z)$ is internally stable and gives a positive γ for all proper controllers, $K(z)$ can be expressed as

$$\|T_{z,w}(z)\|_\infty < \gamma. \tag{13}$$

2.3. Hybrid control structure

In order to promote the convergence speed and increase robust performance in a control system, a hybrid controller is proposed for AVC. The structure combines an adaptive feedforward using the FXLMS algorithm with a feedback using the H_∞ synthesis theory. The composite configuration of the hybrid system is shown in Fig. 5. The value $x(n)$ is primary signal, $y(n)$ is the control signal, and $d(n)$ is the disturbance signal as calculated in the feedback controller. The error signal $e(n)$ is measured by an accelerometer, utilized to compensate the tracking ability of the adaptive controller, and also fed through the feedback controller to obtain an optimal output from the secondary source. The hybrid robust controller is also designed by using the internal model method. An equivalent block diagram of the proposed hybrid system is shown in Fig. 6. The value $W(z)$ is the adaptive controller, $G_{IS}(z)$ is the internal model system of the feedback controller, $y(n)$ is the adaptive controller output signal, and $S(z)$ is the secondary path function. The close-loop function $G_{IS}(z)$ is expressed as

$$G_{IS}(z) = \frac{I(z)S(z)}{1 + I(z)S(z)}. \tag{14}$$

In the proposed design, the transfer function $G_{IS}(z)$ is used to increase the robustness and convergence speed in a system with plant uncertainty.

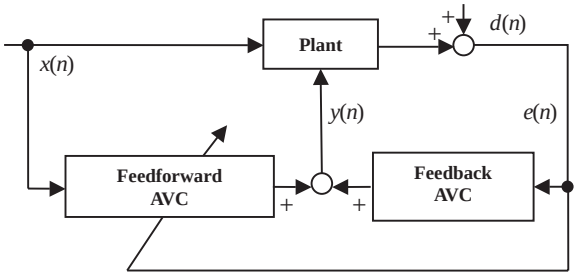

Fig. 5. Hybrid AVC system which is a combination of adaptive AVC and fixed feedback AVC.

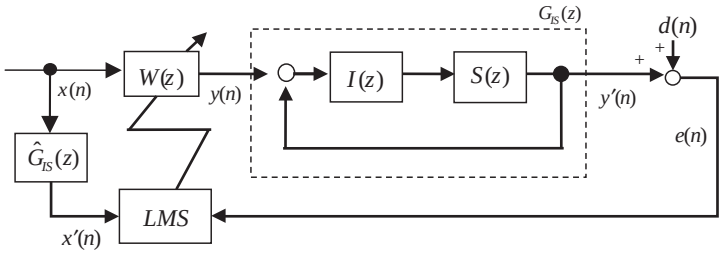

Fig. 6. Equivalent block diagram of a hybrid control system.

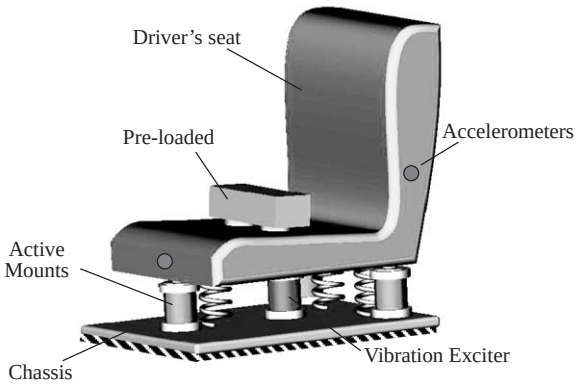

Fig. 7. Schematic of experimental device.

3. Implementation and experimental verification of control systems

3.1. Experimental set-up

The experimental set-up for an active vibration control system in a driver's seat is depicted in Fig. 7. The experimental system is composed of a seat, a vibration generator, three active mounts and three accelerometers on the seat. The mass of the seat and preloaded of driver is 60 kg. This seat is supported by three active mounts and three passive springs. A vibration generator located in the center of the seat is used to generate the periodic vibrations for simulating vibration from the engine or road conditions. The feedback error signals are obtained from three accelerometers (PCB model 353B15) and a monitor by a dynamic signal analyzer (HP35665A). The controllers are implemented on a TMS320C32 DSP equipped with four 16-bit analog I/O channels. The DSP sampling rate is set at 1 kHz in the experiments. The experimental setup is further depicted in Fig. 8. The dashed line from the function generator to the A/D convert interface indicates the reference signal source. In the case of H_∞ feedback control, the controller does not have any reference input signal which can be obtained for a control algorithm.

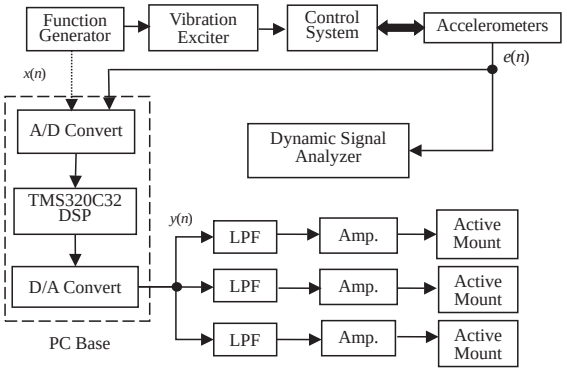

Fig. 8. Experimental arrangement of active control for driver's seat system.

3.2. Experimental results and comparison

To verify the three control algorithms, the first experiment was conducted by using a traditional adaptive controller with the FXLMS algorithm applied to the experimental seat. The frequency response function and the impulse response function of the controller are shown in Fig. 9. The frequency of the vibration source was set at 10 Hz, 20 Hz, 30 Hz and broadband random excitation because the human is the most sensitive to vertical vibration of 0–30 Hz. The AVC result using this adaptive control algorithm is shown in Fig. 10(a). The average attenuation of real-time control in the 20 Hz vibration source of the three error sensors achieved 5.5 dB. Care should be taken to choose the step size value μ and the length of the least mean squares (LMS) order. In general, a large μ guarantees the tracking capability of the algorithm; however, this capability is reduced when the mean-square-error (MSE) is excessively large. By contrast, a small μ will affect the tracking capability and the convergence speed. Therefore, the selection of the optimal convergence factor in an adaptive filter is important. The length of the LMS order is related to the calculation of the capacity of the DSP.

In the secondary experiment, a feedback structure with an H_∞ algorithm was implemented. By relying on the realization of weight functions and the identification of a weighted plant, a 21×21 matrix was computed by using commercial software. The parameters of the lower bound ($\gamma_{\min}$) and the upper bound ($\gamma_{\max}$) were chosen as 1 and 2.5; the tolerable coefficient on the terminated gamma value was chosen as 0.001. The frequency and impulse response functions of the controller are shown in Fig. 11. The experimental result from using feedback H_∞ theory in the 20 Hz vibration source is shown in Fig. 10(b). The vibration attenuation is achieved about 3.3 dB in real-time control.

In order to examine the performance of the proposed hybrid controller, the experiments were conducted in the same conditions. The experimental results indicated that the proposed control system is achieved 11.1 dB vibration attenuation at the same frequency, as shown in Fig. 10(c). The attenuation performance of the three control methods is summarized in Table 1. Obviously, the results indicate that the hybrid H_∞ controller has the best performance in the experimental investigation. In practical implementation, the hybrid H_∞ controller also exhibited a much faster

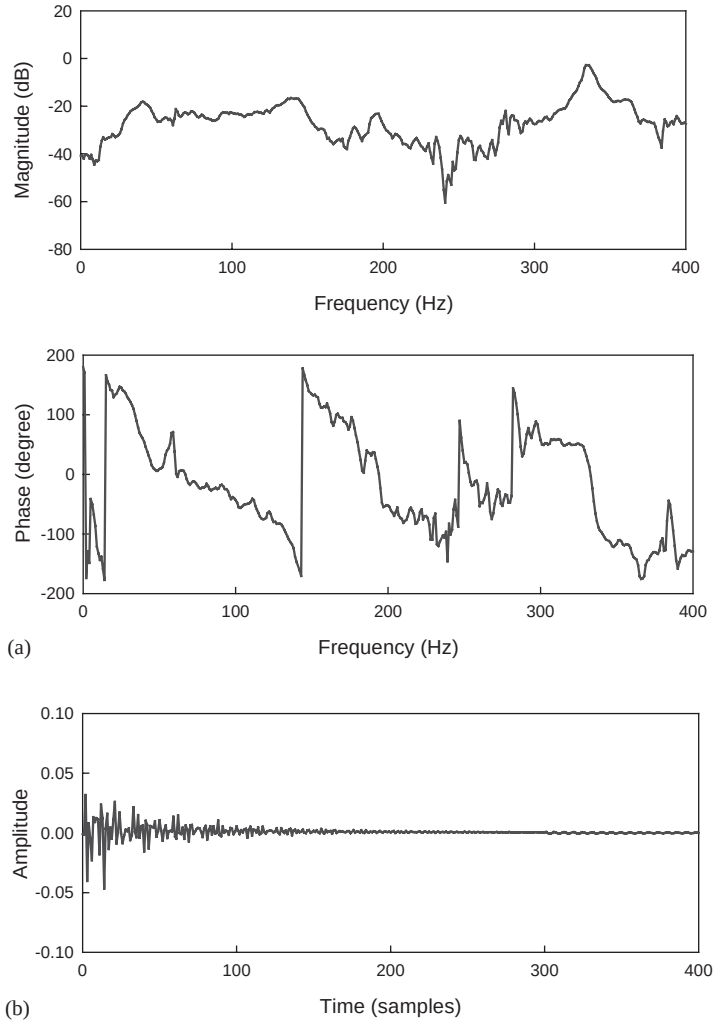

Fig. 9. Adaptive controller implementation. (a) Frequency response function; (b) impulse response function.

convergence speed, stability and robustness in the experimental process. The three structures of AVC merely have different characteristics, as summarized in Table 2. An adaptive controller is often used to deal with active control in cases when the reference source is measurable. However, the convergence speed often limits AVC system performance when a vibration source or a control plant is varied seriously. The pure H_∞ feedback controller is often used in difficult cases to detect the properties of the vibration source in the control system. The proposed hybrid controller has the best performance and robustness in implementation.

In order to understand the performance of the three controllers in random broadband vibration source, experiments are also done in the implementation. The results indicate that an adaptive controller with the FXLMS algorithm only achieves little attenuation in broadband range in 0–50 Hz as shown in Fig. 12(a). Fig. 12(b) shows the control performance of feedback controller,

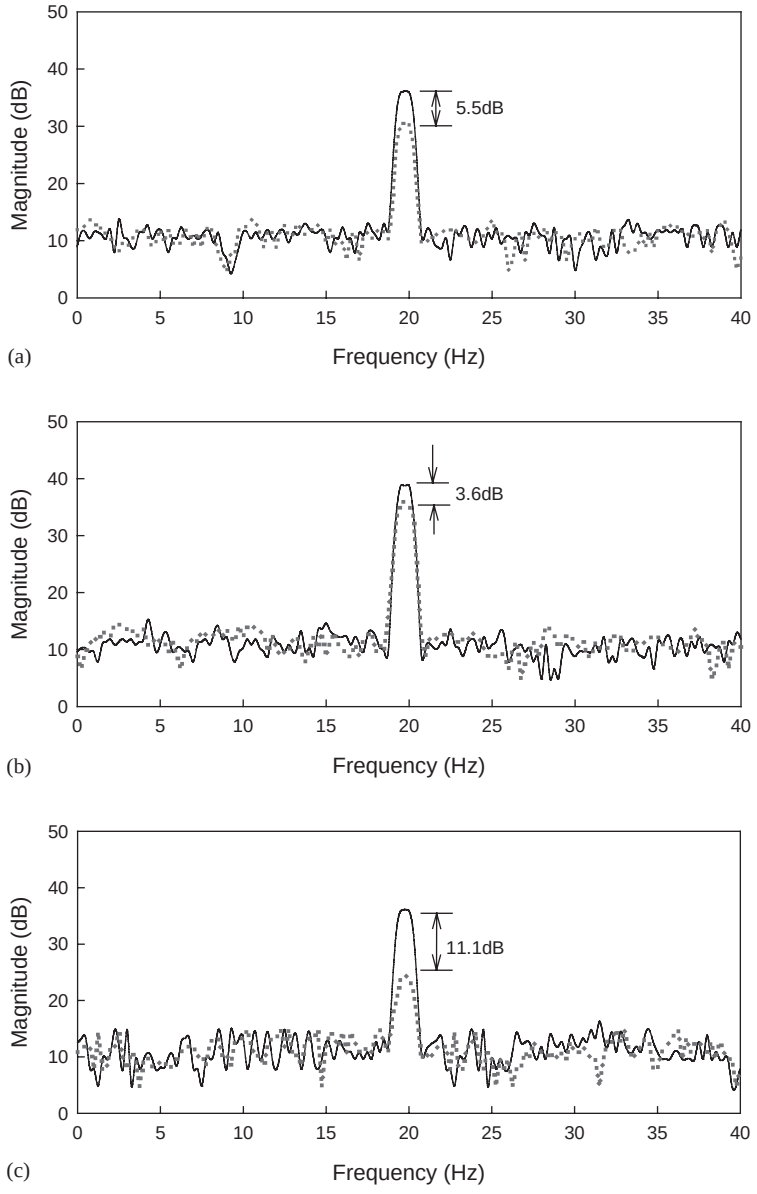

Fig. 10. Experimental results of AVC in 20 Hz vibration excitation. (a) Adaptive control algorithm; (b) H_∞ feedback control; (c) hybrid robust control. Solid line depict control off; dashed line depict control on.

it fails to reduce vibration in broadband vibration. In the third experiment, although significant performance degradation is observed in using proposed control in broadband vibration than periodic vibration. However, the proposed hybrid controller achieves attenuation in some frequency ranges vibration as shown in Fig. 12(c).

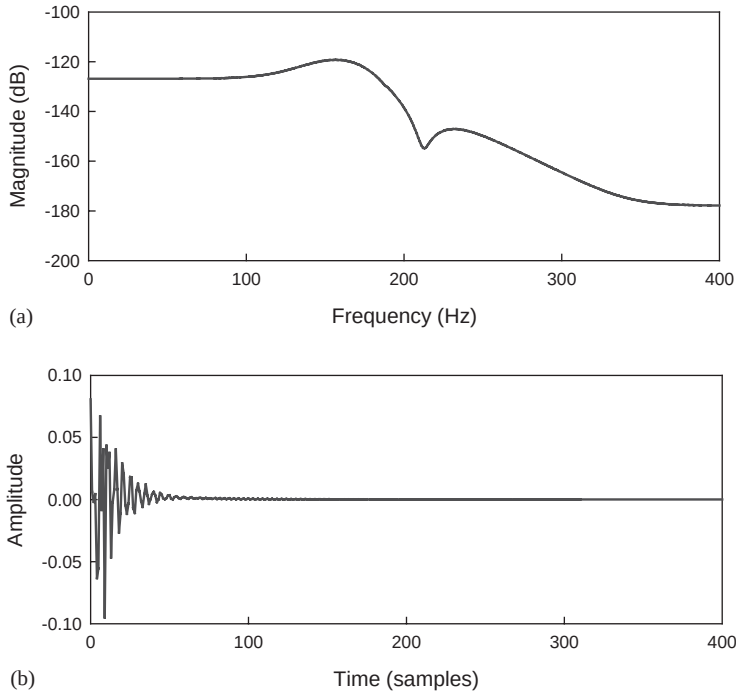

Fig. 11. Fixed H_∞ feedback controller implementation. (a) Frequency response function; (b) impulse response function.

Table 1
Average vibration attenuation in experimental cases

Vibration source	10 Hz	20 Hz	30 Hz
Filtered-x LMS	4.8 dB	5.5 dB	5.5 dB
H_∞ feedback	3.6 dB	3.6 dB	3.3 dB
Hybrid robust	11 dB	11.1 dB	10.4 dB

4. Conclusions

In this study, three active control techniques for reducing undesired small-amplitude vertical vibration in the driver's seat of a vehicle have been investigated. The principles, characteristics and experimental investigation of the proposed controller have been presented. The performance of feedback control is not good as the feedforward control due to the feedback system conducts uncertainty factors that could affect the performance. Thus, hybrid structure consisting of a combination the advantages of the feedforward and feedback structures to increase the robust performance of system. The experimental results indicate that the proposed hybrid robust control structure consisting of a combination of the adaptive controller with the FXLMS algorithm and a

Table 2
Comparison of different control approaches

Control approach	Convergence speed	Control robustness	Adaptability	Stability requirement	System complicacy
Filtered-x LMS	Slow	Medium	Yes	Always stable	Simple
H_∞ feedback	Fast	Medium	No	Could be unstable	Simple
Hybrid robust	Fast	Good	Yes	Always stable	Medium

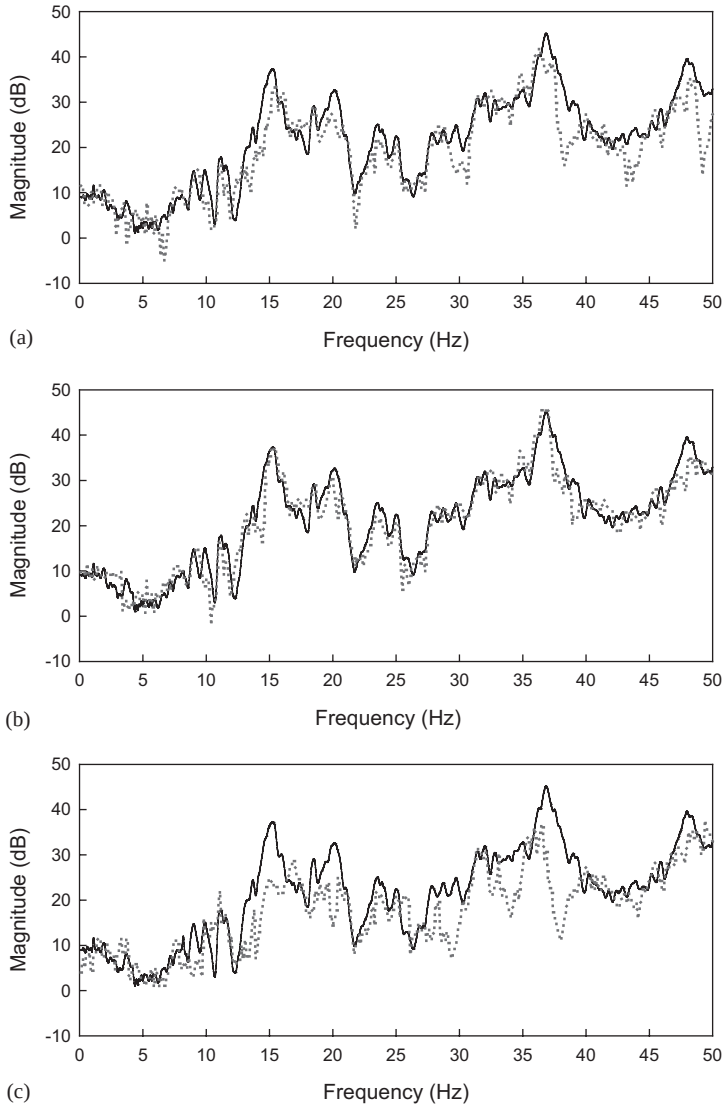

Fig. 12. Experimental results of AVC in random broadband excitation. (a) Adaptive control algorithm; (b) H_∞ feedback control; (c) hybrid robust control. Solid line depicts control off; dashed line depicts control on.

feedback structure with robust synthesis theory achieves fast convergence and superior performance. However, as a limitation of the proposed method, its performance may become degraded if the vibration source is a random broadband vibration. Future design research should focus on the parallel development of a semi-active vibration control such as ER or MR dampers for improving broadband vibration performance and high-amplitude vibration in the driver's seat.

Acknowledgements

The study was supported by the National Science Council of Taiwan, the Republic of China, under project number NSC-90-2745-P-212-003.

The authors also wish to express appreciation to Dr. Cheryl Rutledge for her editorial assistance.

References

[1] G.S. Paddan, M.J. Griffin, Effect of seating on exposures to whole-body vibration vehicles, *Journal of Sound and Vibration* 253 (2002) 215–241.

[2] X. Wu, S. Rakheja, Analyses of relationships between biodynamic response functions, *Journal of Sound and Vibration* 192 (1999) 595–606.

[3] H. Jang, M.J. Griffin, Effect of phase, frequency, magnitude and posture on discomfort associated with differential vertical vibration at the seat and feet, *Journal of Sound and Vibration* 229 (2000) 273–286.

[4] M. Demic, J. Lukic, Z. Milic, Some aspects of the investigation of random vibration influence on ride comfort, *Journal of Sound and Vibration* 253 (2002) 109–129.

[5] J. Alony, S. Sankar, A new concept in semi-active vibration isolation, *American Society of Mechanical Engineers* 109 (1987) 242–247.

[6] X. Wu, M.J. Griffin, A semi-active control policy to reduce the occurrence and severity of end-stop impacts in a suspension seat with an electrorheological fluid, *Journal of Sound and Vibration* 203 (1997) 781–793.

[7] M. C. David, US Patent (1997) 5652704.

[8] C.Q. Howard, S.D. Snyder, C.H. Hansen, Calculation of vibratory power transmission or use in active vibration control, *Journal of Sound and Vibration* 233 (2000) 573–585.

[9] L.R. Miller, M. Ahmadian, C.M. Nobles, D.A. Swanson, Modeling and performance of an experimental active vibration isolator, *American Society of Mechanical Engineers Journal of Vibration and Acoustics* 117 (1995) 272–278.

[10] M.D. Jenkins, P.A. Nelson, R.J. Pinnington, S.J. Elliott, Active isolation of periodic machinery vibrations, *Journal of Sound and Vibration* 166 (1993) 117–140.

[11] J.D. Wu, M.R. Bai, Application of feedforward adaptive active noise control for reducing blade passing noise in centrifugal fans, *Journal of Sound and Vibration* 239 (2001) 1051–1062.

[12] S.M. Kuo, D.R. Morgan, *Active Noise Control Systems: Algorithms and DSP Implementations*, Wiley, New York, 1996.

[13] C.R. Fuller, S.J. Elliott, P.A. Nelson, *Active Control of Vibration*, Academic Press, New York, 1997.

[14] M.R. Bai, H. Chen, A modified H_2 feedforward active control system for suppressing broadband random and transient noises, *Journal of Sound and Vibration* 198 (1996) 81–94.

[15] M.R. Bai, D.J. Lee, Implementation of an active headset by using the H_∞ robust control theory, *Journal of the Acoustical Society of America* 102 (1997) 2184–2190.